Scientific Research Publishing

Advances in Aerospace Science and Technology, 2024, 9, 10-27
https://www.scirp.org/journal/aast
ISSN Online: 2473-6724
ISSN Print: 2473-6708

Derivation of a Revised Tsiolkovsky Rocket Equation That Predicts Combustion Oscillations

Zaki Harari

Novelant Scientific Research Inc., Toronto, Canada
Email: zaki.harari@novelant.com

How to cite this paper: Harari, Z. (2024) Derivation of a Revised Tsiolkovsky Rocket Equation That Predicts Combustion Oscillations. *Advances in Aerospace Science and Technology*, **9**, 10-27.
https://doi.org/10.4236/aast.2024.91002

Received: January 19, 2024
Accepted: March 11, 2024
Published: March 14, 2024

Abstract

Our study identifies a subtle deviation from Newton's third law in the derivation of the ideal rocket equation, also known as the Tsiolkovsky Rocket Equation (TRE). TRE can be derived using a 1D elastic collision model of the momentum exchange between the differential propellant mass element (dm) and the rocket final mass ($m1$), in which dm initially travels forward to collide with $m1$ and rebounds to exit through the exhaust nozzle with a velocity that is known as the effective exhaust velocity ve. We observe that such a model does not explain how dm was able to acquire its initial forward velocity without the support of a reactive mass traveling in the opposite direction. We show instead that the initial kinetic energy of dm is generated from dm itself by a process of self-combustion and expansion. In our ideal rocket with a single particle dm confined inside a hollow tube with one closed end, we show that the process of self-combustion and expansion of dm will result in a pair of differential particles each with a mass $dm/2$, and each traveling away from one another along the tube axis, from the center of combustion. These two identical particles represent the active and reactive sub-components of dm, co-generated in compliance with Newton's third law of equal action and reaction. Building on this model, we derive a linear momentum ODE of the system, the solution of which yields what we call the Revised Tsiolkovsky Rocket Equation (RTRE). We show that RTRE has a mathematical form that is similar to TRE, with the exception of the effective exhaust velocity (ve) term. The ve term in TRE is replaced in RTRE by the average of two distinct exhaust velocities that we refer to as fast-jet, vx_1, and slow-jet, vx_2. These two velocities correspond, respectively, to the velocities of the detonation pressure wave that is vectored directly towards the exhaust nozzle, and the retonation wave that is initially vectored in the direction of rocket propagation, but subsequently becomes reflected from the thrust surface of the combustion chamber

to exit through the exhaust nozzle with a time lag behind the detonation wave. The detonation-retonation phenomenon is supported by experimental evidence in the published literature. Finally, we use a convolution model to simulate the composite exhaust pressure wave, highlighting the frequency spectrum of the pressure perturbations that are generated by the mutual interference between the fast-jet and slow-jet components. Our analysis offers insights into the origin of combustion oscillations in rocket engines, with possible extensions beyond rocket engineering into other fields of combustion engineering.

Keywords

Tsiolkovsky Rocket Equation, Ideal Rocket Equation, Rocket Propulsion, Newton's Third Law, Combustion Oscillations, Combustion Instability

1. Introduction

Konstantin Tsiolkovsky, a Russian rocket scientist, in his publication of 1903 titled "Study of outer space by reaction devices" [1] introduced the mathematical equation that governs the dynamics of rocket propulsion. Tsiolkovsky's derivation leads to what became known as the Tsiolkovsky Rocket Equation (TRE), the ideal rocket equation, or the classical rocket equation, which appears as the solution of a differential equation that is based on the principles of conservation of linear momentum (referred to henceforth simply as momentum) prescribed by Newtonian mechanics. This is the derivation procedure that continues to be taught nowadays in standard textbooks related to rocketry and astronautics [2]-[7].

However, our study shows that Tsiolkovsky's derivation of the equation contains an incomplete application of Newton's third law of classical mechanics. This shortcoming has remained unnoticed over the years. Let us first explore the shortcoming.

The basic principle that is used for deriving TRE can be expressed as: "*The propulsive force derives from momentum changes that originate from ejecting propellant at high velocities*..." [6]. While this statement itself is noteworthy, let us explore the significance of isolating the combustion and propulsion phases of the rocket propulsion problem, and test separately whether the dynamic model that was used to derive TRE is indeed compliant with Newton's third law in each of these two phases.

TRE can be derived using a 1D elastic collision model of the momentum exchange between the differential propellant mass element (dm) and the rocket final mass ($m1$), in which dm initially travels forward to collide with $m1$ and rebounds to exit through the exhaust nozzle with a velocity that is known as the effective exhaust velocity ve. We show below that such a model does not explain how dm was able to acquire its initial forward velocity without the support of a

reactive mass traveling in the opposite direction immediately after combustion but prior to the collision of *dm* with the rocket. Therefore, this model assumes that *dm* remains as a whole particle after combustion, undergoes momentum exchange with the rocket as a whole particle, and gets ejected through the exhaust nozzle also as a whole particle, which violates Newton's third law by omission.

An alternative derivation of TRE that considers *m*1 as the reactive mass and *dm* as the ejected active mass also does not explain the source of the force that repels *dm* away from *m*1, and does not explain that this backward motion of *dm* is indeed the rebound of an initial forward motion of *dm* generated by the reactive support of a separate particle traveling in the opposite direction. Such a TRE model also is unable to comply with a strict application of Newton's third law.

We will show below that in the ideal 1D rocket model that we employ in this work, under the geometric confinement constraints that mimic the combustion chamber of an ideal rocket, the propellant combustion process will result in intra-particle decomposition of the differential mass element *dm*, generating an identical pair of sub-particles each with mass *dm*/2, which we show is a combustion model that complies with Newton's third law of equal action and reaction. We will also show that the rocket propulsion phase incorporates the two co-generated sub-particles, each playing a different role in an integrated dynamic model.

Below we present the derivation of a revised version of the ideal rocket equation that strictly complies with Newton's third law in both the combustion and propulsion phases, and discuss the significance of rectifying the original Tsiolkovsky derivation to show how combustion oscillations are generated from the revised model. The analysis and results presented below are based on non-relativistic classical mechanics.

2. Methods

2.1. Propellant Combustion and Newton's Third Law

Let us first revisit Newton's third law of motion, as documented in The Principia—Mathematical Principles of Natural Philosophy [8]. Newton wrote (translated from Latin): "*Law* 3. *To any action there is always an opposite and equal reaction; in other words, the actions of two bodies upon each other are always equal and are opposite in direction.*" This implies that if there exists an action force that causes a massive particle to change its state of motion in a given direction, then there will always exist a reaction force that causes another massive particle (or equivalent ensemble of particles) to change its state of motion in the opposite direction. This powerful equilibrium law further implies that all forces of action and reaction must coexist at a given instant of co-application of the forces, which implies that a force cannot exist as a solitary action or solitary reaction without a matched force acting in the opposite direction. We will use the above theoretical foundation to further show how the combustion of a solitary differential mass of propellant is able to convert and project its internal

chemical potential energy into the kinetic energy of a pair of sub-particles traveling in opposite directions, in compliance with Newton's third law. As a side note, it is worth observing that in the familiar equation of the kinetic energy *KE* of a massive particle that is expressed as $KE = (1/2) \cdot m \cdot v^2$, the 1/2 multiplier is indeed a manifestation of the bifurcation of the original potential energy of the particle whole into its active and reactive sub-components at the instant of co-generation, which is a direct consequence of Newton's third law.

To develop the conceptual model of the conversion of propellant potential energy into kinetic energy, let us first conduct a thought experiment. Let us imagine that a rocket engine combustion chamber is modeled as a hollow tube carrying a solitary propellant of differential mass *dm*, modeled as a homogeneous spherical mass, traveling at a constant velocity *v* relative to an observer's reference frame. Now, let us suppose that the differential propellant mass *dm* that is initially placed at the conceptual center of the combustion chamber undergoes combustion and uniform spatial scattering outwards from this center. We note that the geometry of the cylindrical structure of the hollow tube constrains the combusted propellant gases to become channeled and travel either in the forward propulsive direction, or rearward exhaust direction. It is worth noting that the gas particles that are directed into the lateral wall of the combustion chamber will become reflected and redirected to either the forward or rearward directions. The magnitude of the resultant momentum carried by each component of the combusted propellant must be equal in the two axial directions of propagation, as prescribed by Newton's law of equal action and reaction. We also deduce that the action-reaction pairing at the microscopic level will aggregate into a macroscopic bifurcation of the ensemble of gas particles into two equal macro sub-particles each of mass *dm*/2, which is a mathematical construct required for differential analysis. The bifurcation of mass is also a direct consequence of the application of the principle of conservation of mass [9], where we know from geometry that when the combusted propellant mass is partitioned symmetrically inside a hollow tube, then the two bilaterally symmetric components of the exhaust gases must be of equal mass.

Based on the above, we arrive at our first working postulate:

Postulate 1. *When a homogeneous spherical differential mass of propellant is combusted inside a hollow tube that permits unimpeded expansion only in two diametrically opposite axial directions, then the mass of the combusted propellant will be bifurcated into two components of equal mass.*

Let us now consider a second thought experiment to frame the scientific basis of our planned analysis. Imagine a rocket moving through free space, propelled by the combustion of a propellant having differential mass *dm* inside its combustion chamber. Let us focus on a specific scenario within this rocket. At the center of the combustion chamber, there is a bullet consisting of two equal masses (see Postulate 1): the projectile (*dm*/2) and the cartridge case (*dm*/2).

Now, let us remotely trigger the bullet to fire in the direction of the rocket's

intended motion. As per Newton's third law, the action of the detonating charge propels the projectile in the forward direction, being supported by the reaction of the cartridge case moving in the backward direction.

Let us pause to ponder the following. The original derivation of TRE assumes that the entire differential mass dm travels forward as a single unit, and becomes reflected from the thrust surface (injector plate) again as a single unit, after imparting momentum to the rocket mass. This is equivalent to a two-body elastic collision problem. Such a conceptual model is unable to explain how the differential propellant mass dm was able to acquire its initial momentum without reacting against another mass traveling in the opposite direction. If indeed it is assumed that the source of the initial momentum of dm is a reaction with another mass element dm that was made to travel in the opposite direction, then we arrive at the conclusion that the initial pre-combustion propellant must have a total mass $2{\cdot}dm$. If $2{\cdot}dm$ is then mapped to dm for mathematical consistency, we arrive at the same bifurcation model that we used in our derivation of RTRE in which one particle of mass dm generates a sub-particle pair each with mass $dm/2$. In summary, to adhere to Newton's third law at the microscopic level, it is essential to have a differential mass pair of action and reaction, simultaneously created during propellant combustion. Once the pair has been created, the particle that travels in the forward direction will collide with the thrust surface and impart momentum to the rocket mass. This is the order of the cascade of events from the microscopic scale of combustion to the macroscopic scale of momentum exchange.

We now map our above thought experiment to the physical combustion of an element of propellant inside a conventional rocket combustion chamber, and define the cartridge case as the analog of the detonation pulse, and the projectile as the analog of the retonation pulse. We adopt the convention of using the term detonation for the pulse that is directed towards the open end of the chamber, and the term retonation for the pulse that travels to the closed end (the thrust surface). Such a bifurcation of combustion gases into detonation-retonation pulses has been verified experimentally in the published literature [10].

Also, since the projectile and cartridge case have equal mass (Postulate 1), their velocities will be identical but in opposite directions, which is a requirement of the momentum equilibrium condition derived from Newton's third law. Let us denote the projectile's velocity as $+vx_1$ and the cartridge casing's velocity as $-vx_1$.

Based on the above, we arrive at our second working postulate:

Postulate 2. *When a homogeneous spherical differential mass of propellant is combusted inside a hollow tube that permits unimpeded expansion only in two diametrically opposite axial directions, then the magnitude of the velocities of the bifurcated equal masses will be identical, and vectored in opposite axial directions.*

Mapping our thought experiment onto the case of a real rocket combustion chamber, we see that the projectile collides with the thrust surface of the rocket

combustion chamber, while the cartridge case is already moving away and does not make contact with the thrust surface. At the moment of projectile to thrust surface collision, an equilibrium of forces occurs between the projectile and the rocket, causing the projectile to induce an acceleration on the rocket which has a mass $m1$.

We can now apply momentum conservation to determine that, after the propulsion phase, the increase in momentum of the rocket must balance the decrease in momentum of the projectile.

After the collision, the projectile rebounds from the thrust surface, reversing its direction and traveling backward. It then exits the exhaust nozzle with a velocity of $-vx_2$. Due to the loss of some momentum during the collision with the thrust surface, the absolute value of $-vx_2$ is smaller than that of $+vx_1$.

We conclude from application of Postulate 1 and Postulate 2 that when a rocket is propelled by the combustion (or detonation) of a solitary propellant particle, two particles with different velocities emerge from the exhaust nozzle. This bifurcation in exhaust velocity occurs because of the application of Newton's third law during the combustion phase. It is important to note that only one-half of the bullet's mass actively interacts with the rocket thrust surface. This seemingly counter-intuitive result becomes clear when we consider a scenario where the bullet's initial position is entirely outside the rocket's combustion chamber, and it is then fired into the chamber. The resulting change in rocket velocity would be the same as if the bullet's initial position were entirely inside the chamber. However, in this case, it is evident that only one particle with a mass of $dm/2$ exits the exhaust nozzle after collision and rebound.

Now, the question arises: How can we determine the change in velocity (dv) of the rocket? To calculate dv, we need to know either vx_1 or vx_2, which we will refer to as the fast-jet and slow-jet components of the exhaust, respectively. If we use the TRE model and choose to ignore the bifurcation and instead equate vx_1 and vx_2 individually to the effective exhaust velocity (ve), the effect is to attribute one average exhaust velocity value ve to the entire propellant mass element dm, ignoring the conditions imposed by Newton's third law of motion, as shown above. This averaging approximation is the analytical approach that was used in the derivation of the original TRE, which has the effect of obscuring the underlying mechanism which we will show below is responsible for generating combustion oscillations.

What more evidence is there in the literature for the bifurcation of the by-products of propellant combustion? Let us start with a direct quote from a recent publication, "... *when a detonation pulse is formed, an explosion pulse propagating backward is formed at the same time, which is called retonation pulse*" [11]. This laboratory study used a horizontal tube with an ammonia/oxygen mixture acting as the propellant.

Perhaps one of the earliest works to report the retonation phenomenon in rocket engines identifies the phenomenon as a process that has been initiated by a point explosion [12]. There are studies suggesting that combustion instability is caused by pressure oscillations in the rocket engine combustion chamber [13]

[14], as a consequence of which the dreaded pogo oscillation has been known to cause catastrophic failure in rockets [15] [16]. From a related field, it is reported that when a flame is ignited in the middle of an open tube, the flame propagates in both directions [17]. Another experimental study used a tube that was closed at one end, and found oscillation frequencies that were close to the fundamental acoustic mode, suggesting that the oscillations are primarily triggered by initial flame motion [18]. The above works indicate that there is a phenomenon of backward propagation at the point of propellant combustion, which has been observed experimentally and interpreted as the initiation of turbulent flow [19]. On the basis of our discussion above and the analysis below, we conclude that the detonation-retonation phenomenon and the related bifurcation of the exhaust gases is an essential consequence of the strict application of Newton's third law of equal action and reaction.

2.2. Derivation of the Revised Tsiolkovsky Rocket Equation (RTRE)

We now proceed to analyze the dynamics of the propellant combustion and rocket propulsion problem, leading to the derivation of the Revised Tsiolkovsky Rocket Equation (RTRE).

There are three phases: the initial phase where the propellant has not undergone combustion; the combustion phase where the propellant has undergone combustion but where there is yet no interaction with the thrust surface, therefore the rocket has not undergone any propulsion; the propulsion phase which is immediately after the forward component of the propellant has collided with the thrust surface and caused the rocket to gain a differential velocity *dv*, while the propellant has lost some of its momentum.

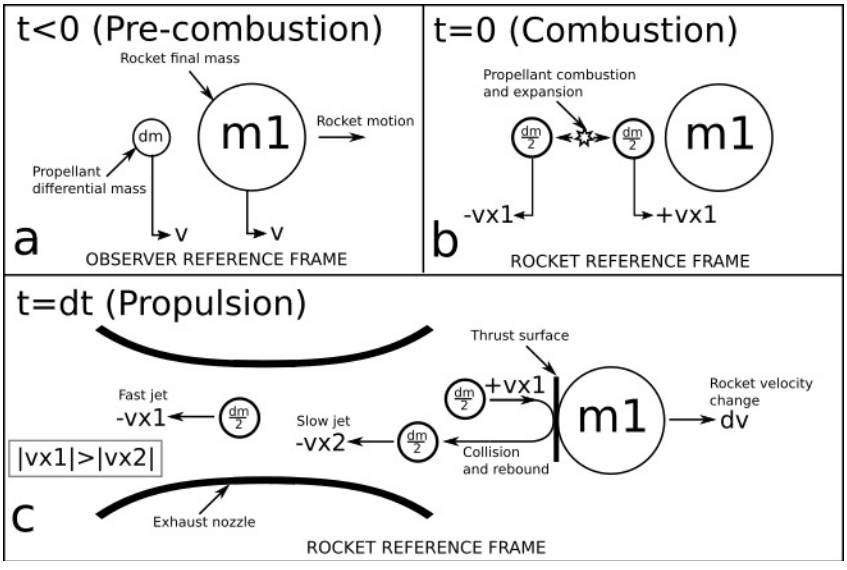

Figure 1. The proposed rocket propulsion model a) Initial state of motion at $t = 0$, b) State of motion during propellant combustion at time $t = 0$, c) State of motion after rocket propulsion at $t = dt$.

Figure 1 shows the basic components that are required for analyzing the dynamics of the rocket—propellant system. Referring to Figure 1(a), the total mass of the rocket at time $t = 0$ prior to combustion is $m1 + dm$, where $m1$ is the final mass of the rocket, and dm is the differential mass of the propellant that will be ejected from the exhaust nozzle after the end of the combustion-expansion and propulsion cycle at time $t = dt$, where dt is differential time. Before combustion, as shown in Figure 1(a) dm is traveling at the same velocity v as the rocket. Immediately after combustion, as shown in Figure 1(b), dm will become bifurcated into its two sub-particles each of mass $dm/2$. In Figure 1(c) we see that the active component of $dm/2$ collides with the thrust surface of the combustion chamber, and rebounds to travel backward to be ejected from the exhaust nozzle with the slow jet velocity $-vx_2$. The collision with the thrust surface propels the rocket in the forward direction with a change of velocity of dv, the change of velocity being identical both in the rocket and observer reference frames.

We are now ready to analyze the dynamics of the propellant-rocket system, and determine the rocket velocity change dv.

By definition, the initial mass of the rocket including the uncombusted propellant is m_0, such that $m_0 = m_1 + dm$, where m_1 is the final mass of the rocket, and dm is the differential mass of the propellant. The initial velocity of the rocket is v_0. We continue our analysis in the rocket reference frame. Our 1D coordinate system is such that the positive axis points in the direction of rocket motion.

In the initial phase, for the combined rocket and propellant system, the total momentum (P_0) is the sum of the rocket initial momentum (P_{r0}) and the propellant initial momentum (P_{p0}) in the rocket reference frame:

$$P_0 = P_{r0} + P_{p0} = 0 \tag{1}$$

In the combustion phase, the total momentum (P_1) is the sum of the rocket combustion momentum $P_{r1} = 0$ and the forward half of the propellant combustion momentum $P_{p1} = (dm/2) \cdot vx_1$:

$$P_1 = P_{r1} + P_{p1} = \frac{dm \cdot vx_1}{2} \tag{2}$$

In the propulsion phase, the total momentum (P_2) is the sum of the rocket propulsion momentum $P_{r2} = m_1 \cdot dv$, and the momentum of the forward half of the propellant after it has collided with the thrust surface and rebounded to exit through the exhaust nozzle with velocity $-vx_2$, such that $P_{p2} = -(dm/2) \cdot vx_2$:

$$P_2 = P_{r2} + P_{p2} = m_1 \cdot dv - \frac{dm \cdot vx_2}{2} \tag{3}$$

For momentum conservation, we equate the total propulsion momentum (P_2) with the total combustion momentum (P_1) to yield the momentum conservation equation, which after simplification becomes:

$$2 \cdot m_1 \cdot dv - dm \cdot vx_2 = dm \cdot vx_1 \tag{4}$$

Before we convert Equation 4 into a differential equation, we express it in dif-

ference equation form by making the substitutions $m_1 = m[n+1]$, $dv = (v[n+1] - v[n])$, $dm = (m[n] - m[n+1])$, noting that dm is conventionally defined as $m0 - m1$ which is the initial mass $m0$ of the rocket at time $[n]$, minus the final mass $m1$ at time $[n+1]$. Finally substituting $(v[n+1] - v[n]) = v'(t)$ and $(m[n] - m[n+1]) = -m'(t)$, we obtain the following ordinary differential equation:

$$2 \cdot m(t) \cdot v'(t) + m'(t) \cdot v_{x2} = -m'(t) \cdot v_{x1} \tag{5}$$

In Equation 5, we note that the sign of the mass derivative has become negative, after conversion from the difference equation as described above.

Equation 5 is an ODE which can be solved with initial conditions $v[0] = v_0$ to yield the rocket velocity v, following which we can obtain the change in velocity $dv = v - v0$:

$$dv = \frac{1}{2} \cdot (vx_1 + vx_2) \cdot \log\left(\frac{m_0}{m_1}\right) \tag{6}$$

Equation 6 is what we call the Revised Tsiolkovsky Rocket Equation (RTRE). We see immediately that RTRE is similar in structure to the Tsiolkovsky Rocket Equation (TRE) shown in Equation 7, where ve is known as the effective exhaust velocity. However, we will retain the RTRE formulation with the two distinct exhaust velocities vx_1 and vx_2 for reasons that will be evident below.

$$dv = ve \cdot \log\left(\frac{m_0}{m_1}\right) \tag{7}$$

2.3. Relationship between the Exhaust Velocities vx_1 and vx_2

Let us now find the relationship between vx_1 and vx_2. We will treat the momentum exchange between the combusted propellant and the rocket as an elastic collision problem. Only one of the two exhaust velocities needs to be known in order to compute the other one and solve the collision problem. We arbitrarily select the velocity vx_1 (fast-jet) as the known quantity, following which we solve the collision problem to compute vx_2 in terms of vx_1. Since the velocity change variable dv is also an unknown variable, we will need to solve two simultaneous algebraic equations to find vx_2 in terms of vx_1 and the mass variables $m0$ and $m1$. The two algebraic equations are the momentum conservation and kinetic energy conservation equations in the rocket reference frame.

The momentum conservation equation (identical to Equation 4) is:

$$\frac{dm}{2} \cdot vx_1 = m \cdot dv - \frac{dm}{2} \cdot vx_2 \tag{8}$$

The kinetic energy conservation equation is:

$$\frac{1}{2} \cdot \left(\frac{dm}{2}\right) \cdot vx_1^2 = \frac{1}{2} \cdot m \cdot dv^2 + \frac{1}{2} \cdot \left(\frac{dm}{2}\right) \cdot (-vx_2)^2 \tag{9}$$

We now solve Equations 8 and 9 simultaneously to obtain an expression for vx_1 in terms of vx_2, after substituting $m = m1$ and $dm = m0 - m1$. Next we di-

vide the vx_1 solution by vx_2 to fsind an expression for the exhaust velocity ratio β_{vx} as:

$$\beta_{vx} = \frac{vx_1}{vx_2} = \frac{m0 + m1}{3 \cdot m1 - m0} \tag{10}$$

3. Results and Discussion

Let us apply the results presented above in a numerical simulation. For the purpose of the following simulation, we will assume an ideal rocket in which we do not consider thermodynamic losses. Also, our analysis focuses exclusively on momentum thrust, disregarding any consideration for pressure thrust, which falls outside the scope of this investigation.

In Table 1, we show sample operational parameters for a rocket that we shall use in a simulation study. The column "*MR*" is the mass ratio defined as $MR = \frac{m0}{m1}$. The column "Δv TRE" represents the velocity change Δv computed using the Tsiolkovsky Rocket Equation (TRE).

Before proceeding with the simulation, given only the parameters of Table 1, we need to find the appropriate values of vx_1 and vx_2 in RTRE that will yield the value of **Δv TRE (m/s)** shown in Table 1. Therefore, by comparing the mathematical form of Equation 5 and Equation 6, we find the following relationship:

$$ve = \frac{1}{2}\left(vx_1 + vx_2\right) \tag{11}$$

Solving simultaneously Equation 11 with Equation 10, we obtain the following:

$$\begin{aligned} vx_1 &= \frac{\left(m_0 + m_1\right) \cdot ve}{2 \cdot m_1} \\ vx_2 &= \frac{\left(3 \cdot m_1 - m_0\right) \cdot ve}{2 \cdot m_1} \end{aligned} \tag{12}$$

We can express vx_1 and vx_2 of Equation 12 in terms of *dm*, given $dm = m_0 - m_1$, to yield:

$$\begin{aligned} vx_1 &= ve \cdot \left(1 + \frac{dm}{2 \cdot m_1}\right) \\ vx_2 &= ve \cdot \left(1 - \frac{dm}{2 \cdot m_1}\right) \end{aligned} \tag{13}$$

We note from Equation 13 that the values of the fast-jet velocity *vx*1 and the

Table 1. Example of a rocket for propulsion simulation study.

*m*0 (kg)	*m*1 (kg)	*MR*	*ve* (m/s)	Δv TRE (m/s)
50000	30000	1.67	2500	2085.18

slow-jet velocity $vx2$ are symmetrical about ve, and their distance from ve is identical to one-half of the ratio between dm and m_1. This yields the interesting property that the difference between $vx1$ and $vx2$ will be minimized when the ratio of dm to m_1 is also minimized. We will address this property below in the context of the discussion about combustion oscillations.

Expanding on our earlier assessment of the derivation of the Tsiolkovsky Rocket Equation, we raise the question regarding the magnitude of the starting forward velocity of the mass element (dm) before it collides with the thrust surface, undergoing reflection and subsequent ejection as exhaust. Our earlier analysis indicates that the forward velocity (vx_1) will be greater in magnitude than the effective exhaust velocity (ve). This suggests the existence of another propellant particle (dm) that will exit the exhaust nozzle at a velocity of magnitude vx_1 before the reflected pair element (dm) also exits at velocity ve. As a result, we see that the total mass of the ejecta must be twice dm. By setting the differential mass element to be redefined as dm by mathematical convention, we conclude that the forward vectored active component of the propellant must be $dm/2$, not dm. We also deduce that the component of the exhaust gases that is reflected from the thrust surface will exit the exhaust nozzle at the velocity $-vx_2$, which is smaller in magnitude than ve. This aligns with the model adopted in the derivation of the Revised Tsiolkovsky Rocket Equation (RTRE), which indeed adheres to Newton's third law.

1D simulation of Pressure Oscillations Generated by Exhaust Bifurcation

Combustion oscillations (instabilities) were a major problem that plagued the design of the F-1 engine for the Saturn V rocket. Such oscillations are generally attributed to turbulent flow and coupling between the chamber acoustics and the flame front.

In order to identify the primary mechanism that generates combustion oscillations, we have derived above the theoretical basis for the occurrence of exhaust velocity bifurcation in the combustion chamber of a rocket engine. We know from Bernoulli's principle that a change in the velocity of a fluid will cause a change in the flow pressure [20]. Therefore, we can deduce that the velocity bifurcation inside the rocket combustion chamber, coupled with repeated cycles of propellant combustion, will set up a flow perturbation which generates a pressure oscillation inside the chamber [21] [22] [23]. There is also experimental and numerical analysis evidence in the literature which indicates that combustion in both an open and closed tube results in the splitting of the combustion flame into forward and rearward components [24]. In this work, it is seen that when the rearward propagating component is reflected from the end of the closed tube it generates a reflected flame that travels forward with a finite delay relative to the forward flame, which is a mechanism that generates turbulent flow.

We will now simulate the pressure oscillations in an ideal rocket combustion chamber, which is modeled as a series of discrete propellant combustion events, with the propellant placed at a nominal distance between the combustion point and the thrust surface, which can be varied as required. We point out that the 1D

simulation results presented in this study are only qualitative, and should not be used in quantitative form for any purpose, including for engine design purposes.

We will use a blast pulse pressure profile (a pulse) that can be approximated by a combination of an exponential decay function and a left-skewed Gaussian, as shown in Equation 14, similar in general shape to the Chapman-Jouguet (CJ) detonation model shown in Ref. [25].

$$p(t) = \mathrm{Exp}\left[-(t-\mathrm{center})^2 \Big/ \left(2\cdot \mathrm{width}^2\right)\right] * \left(1-\mathrm{Erf}\left[-\mathrm{skewness}(t-\mathrm{center}) \Big/ \left(\sqrt{2}\cdot \mathrm{width}\right)\right]\right) \tag{14}$$

In Equation 14, $p(t)$ represents the pressure at time *t*. The function $\mathrm{Erf}(z)$ is the error function. The parameter "center = 0.0006" controls the position of the start of the pulse, "width = 0.001" determines the general width of the pulse, and "skewness = −5" controls the skewness of the pulse. These parameters define the characteristics of the source pulse, which we will use to simulate the combustion oscillations.

Our 1D simulation begins with a spike train comprising the direct pulse (fast-jet with velocity vx_1), followed after a time lag by the reflected pulse (slow-jet with velocity vx_2). We choose to set each spike arbitrarily to a unit amplitude, assuming that the reflection of the forward pulse from the thrust surface will exhibit a reflection coefficient ρ that that we will vary in order to simulate various scenarios. We then create the synthetic pressure trace by the convolution of the source pulse with the spike train, thereby replicating a discrete propellant combustion event. The parameters that we use are not necessarily representative of an actual rocket engine, but are rather selected to illustrate some fundamental concepts that will be discussed below.

In **Figure 2**, we observe a simulated propellant combustion using a combination of fast-jet and slow-jet pressure pulses. The pressure trace is recorded at three different positions along the x-axis: $x = 0$ m, $x = 2$ m, and $x = 4$ m.

At each measurement location, we first observe the arrival of the fast-jet pulse, which travels at a velocity vx_1 and reaches the point at time $t(x) = x/vx_1$. The second arrival is the slow-pulse, which initially moves forward at the high velocity vx_1 from the source to the thrust surface located at a distance of 1 m from the source. After reflection, it travels backward at the slower velocity vx_2 until it reaches the measurement location at distance *x* from the center of combustion.

It is important to note that the composite traces have different shapes due to the varying delay times between the fast-jet and slow-jet arrivals. The time lag between the two arrivals is directly proportional to the distance of the measurement point, and the difference between vx_1 and vx_2.

Additionally, each trace exhibits a distinct frequency spectrum. In particular, the spectrum at $x = 2$ m and $x = 4$ m displays a local peak at approximately 350Hz and 500Hz, respectively. This suggests that understanding the dynamic nature of the spectrum in relation to the location within the combustion chamber is crucial for addressing combustion oscillations effectively.

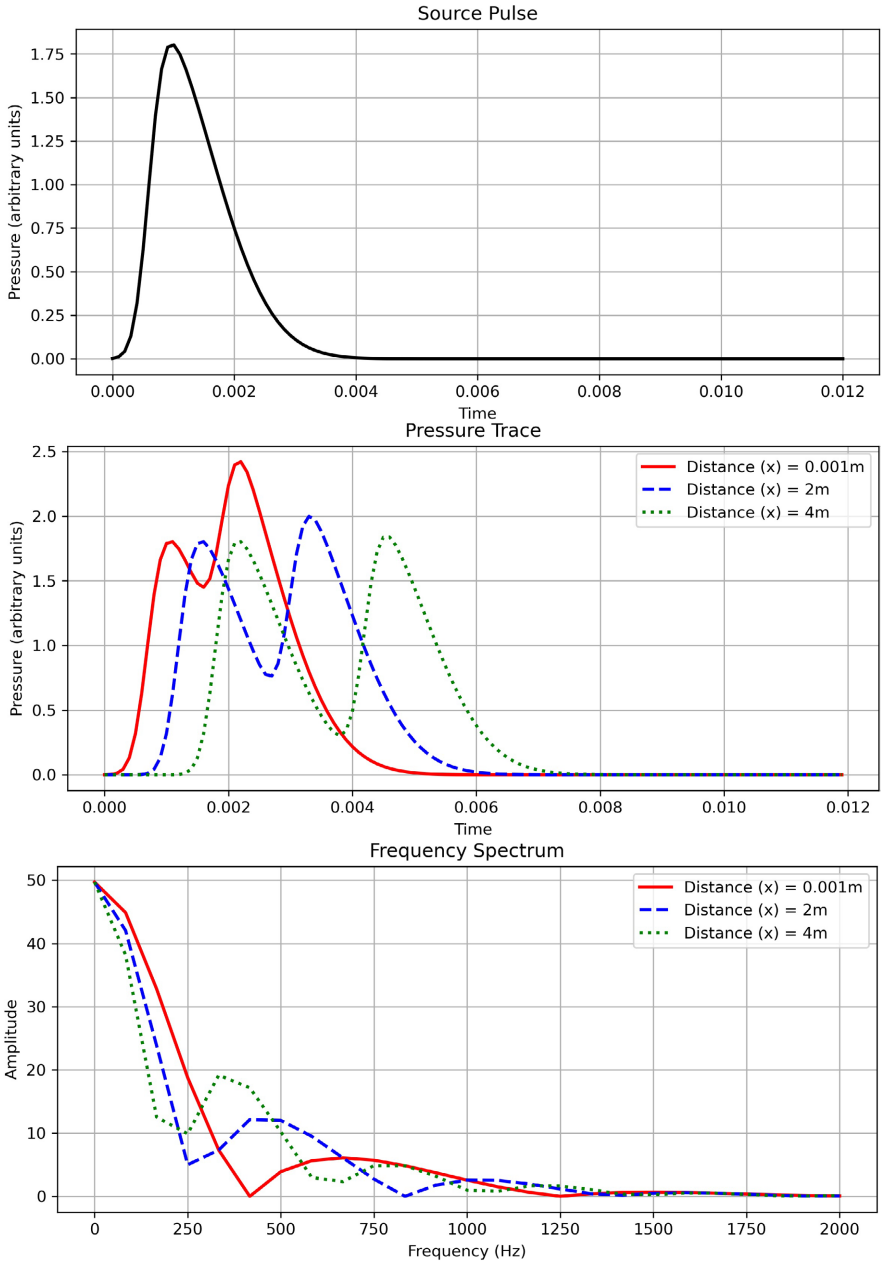

Figure 2. Simulated pressure trace of the combined fast-jet and slow-jet synthetic, as a function of measurement distance (x) relative to point of combustion. The simulated distance between the thrust surface and the point of combustion is chosen to be 1 m, and the reflection coefficient (ρ) of the thrust surface is +1, which implies total lossless reflection.

In **Figure 3**, we present simulated pressure traces for three cases of thrust surface reflection coefficients: $\rho = +1$, $\rho = 0$, and $\rho = -1$. The measurement distance and thrust surface distance are kept constant across all cases.

A reflection coefficient of $\rho = +1$ indicates that the pressure pulse is fully reflected by the thrust surface, with the amplitude, polarity and shape of the reflection being identical to the incident pulse. Conversely, a reflection coefficient of $\rho = -1$ implies a reversed polarity pressure pulse.

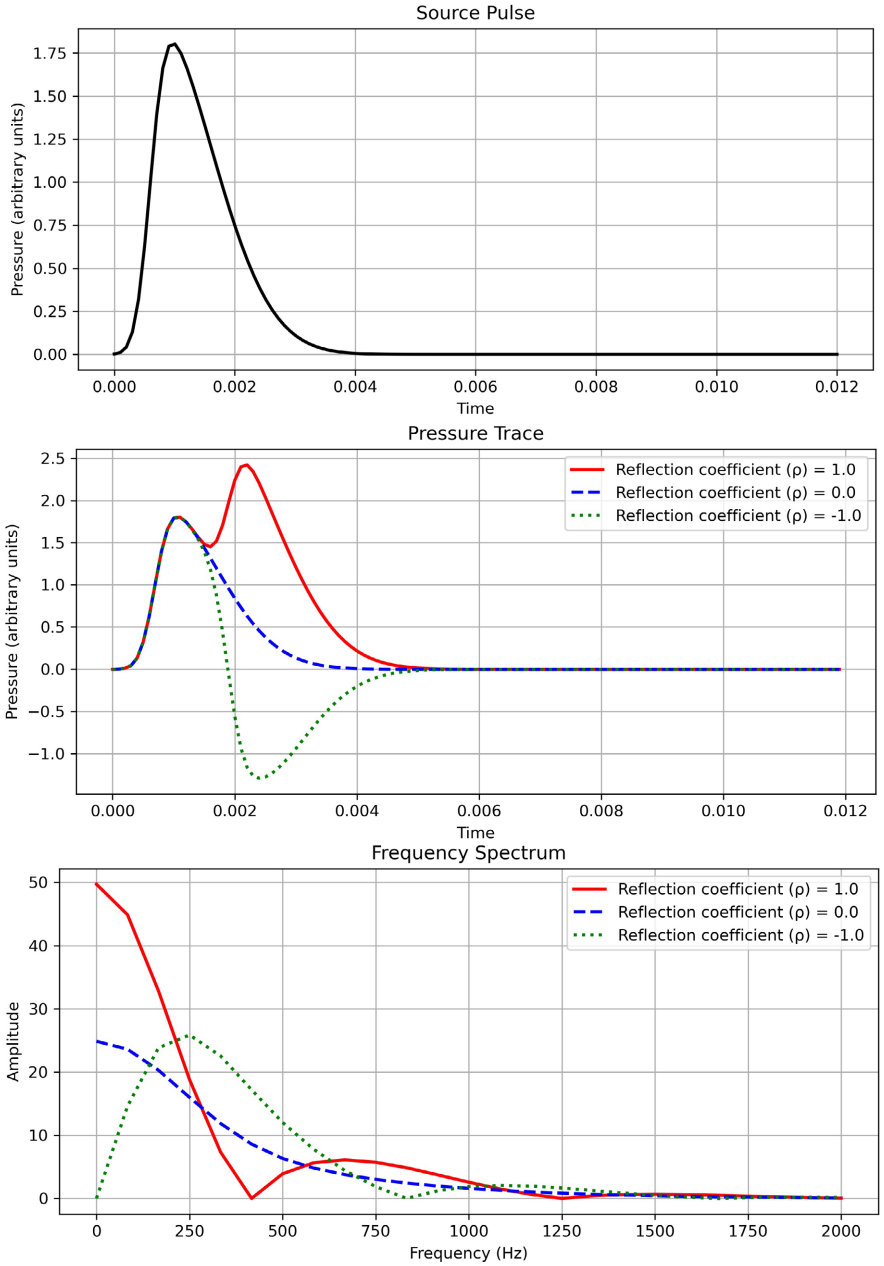

Figure 3. Simulated pressure trace and amplitude spectrum of the combined fast-jet and slow-jet synthetic, as a function of thrust surface reflection coefficient (ρ). The simulated distance between the thrust surface and the point of combustion is 1 m.

Of particular interest is the case where $\rho = 0$, which corresponds to the theoretical case where the thrust surface fully absorbs the reflection of the forward propagating pressure pulse. In this hypothetical case, the pulse may either pass through fully or be absorbed completely. This scenario can be viewed as an idealization of a damping mechanism installed on the thrust surface. Damping techniques have been successfully employed in the design of F-1 rocket engines for the Saturn V, contributing to the mitigation of combustion oscillations [26].

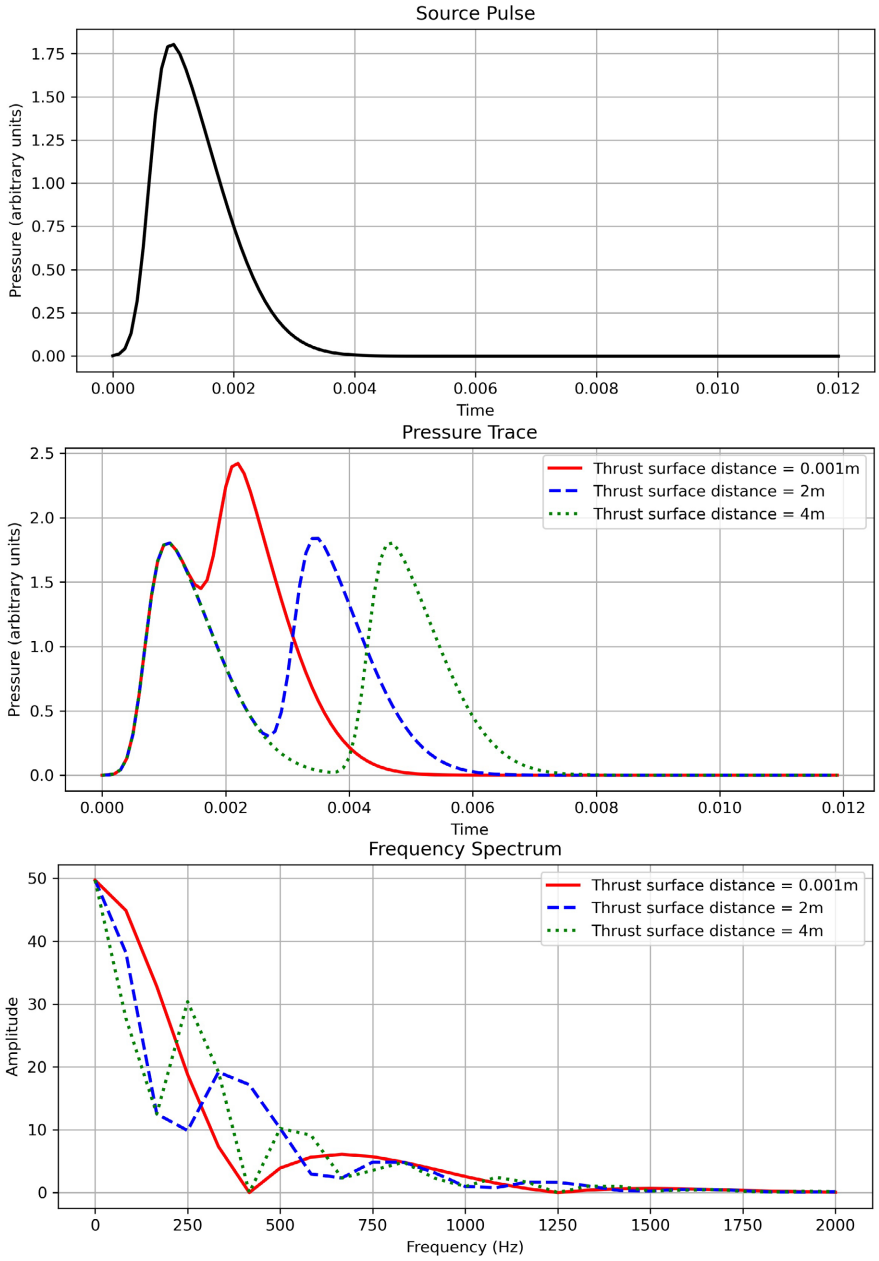

Figure 4. Simulated pressure trace assnd amplitude spectrum of the combined fast-jet and slow-jet synthetic, as a function of thrust surface distance.

In **Figure 4**, we display three simulated pressure traces corresponding to different distances of the thrust surface from the source of combustion, located at x = 0 m. The thrust surface distances are 1 m, 2 m, and 3 m, while the reflection coefficient remains constant at $\rho = +1$.

Comparing **Figure 4** with **Figure 2**, we observe that varying the thrust surface distance has a similar impact on the trace shape and frequency spectrum, to changing the measurement position alone, but with one significant difference. In **Figure 4**, the arrival time and shape of the direct pulse (fast-jet) remain unaltered by the position of the thrust surface, whereas they are influenced by the

position of the measurement location, as shown in Figure 2.

Also, in Figure 2, the arrival times of both the fast-jet and the slow-jet exhibit linear variation with the x-offset. These characteristics of the two jets can be leveraged to optimize the design of the rocket combustion chamber, utilizing the constructive and destructive interference phenomena illustrated using the convolution model presented in this work, and deploying an array of reflectors and dampers that are placed in a suitable pattern over the 3D area of the thrust surface, as a method of mitigating combustion oscillations.

4. Conclusions

We identify a subtle deviation from Newton's third law in the derivation of the well-known Tsiolkovsky Rocket Equation (TRE). We show that the transfer of momentum and kinetic energy from propellant combustion to rocket propulsion involves a bifurcation of the differential mass element dm of the combusted propellant. We show that only the active half of dm interacts with the combustion chamber's thrust surface in an exchange of momentum, while the other reactive half exits the exhaust nozzle without interacting with the thrust surface.

Based on this observation, we derive a rocket equation that we refer to as the Revised Tsiolkovsky Rocket Equation (RTRE). The derived equation has a mathematical structure that is similar to TRE but employs two distinct velocities vx_1 and vx_2 instead of one effective exhaust velocity ve. TRE's use of the effective velocity helps to obscure the presence of a bifurcated exhaust velocity stream, which we show can be modeled to explain the origin of combustion oscillations inside a rocket combustion chamber. We also demonstrate that if vx_1 and vx_2 are unknown, they can be computed to match the available or measured value of dv, with prior knowledge of ve and the mass parameters $m0$ and $m1$.

To investigate the role of the bifurcated exhaust velocity state as a possible origin of combustion oscillations, we conduct a 1D numerical simulation study. By varying the pressure measurement position within the combustion chamber, we observe changes in the pressure wave's frequency characteristics. We note that the position of measurement of the pressure wave has a similar effect to that of varying the distance between the combustion center and the thrust surface. We also simulate the impact of varying the thrust surface's reflection coefficient, finding that it influences the shape and frequency content of the composite pressure wave.

We can also conclude from Equation 13 that the difference between $vx1$ and $vx2$ is proportional to the ratio between dm and m_1. We note that decreasing the difference between $vx1$ and $vx2$ will result in a smaller time lag between the peaks of the detonation and retonation pressure pulses, which is expected to increase the high frequency content of the composite pressure wave, as can be deduced from the results shown in Figure 2 and Figure 4 of our simulation above.

Based on our observations above, we can summarize the basic principle of rocket propulsion as follows: A rocket moves forward when the higher gas pressure inside the combustion chamber exceeds the lower gas pressure at the ex-

haust nozzle. The ejection of gases through the exhaust nozzle provides the necessary support (inertial plug) to maintain the gas pressure inside the combustion chamber. The expulsion of gases through the exhaust nozzle occurs immediately after the generation of gas pressure in the combustion chamber. This gas pressure is the source of the force that propels the rocket forward, contrary to the common belief that rearward mass ejection through the exhaust nozzle causes forward rocket propulsion. In other words, rearward mass ejection is the visible after-effect, not the cause of rocket propulsion.

In conclusion, we show that the results of this study challenge some existing paradigms in the field of rocket engineering. Our study has the objective of contributing to the design of more efficient rocket engines based on the understanding of the fundamental processes that contribute to combustion instability. This study also has the potential to contribute insights to other areas of combustion engineering.

Conflicts of Interest

The author declares no conflicts of interest regarding the publication of this paper.

References

[1] Tsiolkovsky, K.E. (1975) Study of Outer Space by Reaction Devices. https://archive.org/details/nasa_techdoc_19750021068/page/n1/mode/2up

[2] Sutton, G.P. and Biblarz, O. (2016) Rocket Propulsion Elements. John Wiley & Sons, New York.

[3] Taylor, T.S. (2017) Introduction to Rocket Science and Engineering. CRC Press, Boca Raton.

[4] Goodger, E.M. (2013) Principles of Spaceflight Propulsion. Elsevier, Cham.

[5] Curtis, H.D. (2013) Orbital Mechanics for Engineering Students. Butterworth-Heinemann, Oxford. https://doi.org/10.1016/B978-0-08-097747-8.00006-2

[6] Sellers, J.J., Astore, W.J., Giffen, R.B. and Larson, W.J. (2000) Understanding Space: An Introduction to Astronautics. Primis, Hong Kong.

[7] Kluever, C.A. (2018) Space Flight Dynamics. John Wiley & Sons, New York.

[8] Cohen, I.B., Whitman, A. and Budenz, J (1999) The Principia: The Authoritative Translation and Guide: Mathematical Principles of Natural Philosophy. University of California Press, California.

[9] McAllister, S., Chen, J.Y. and Fernandez-Pello, A.C. (2011) Fundamentals of Combustion Processes. Springer, New York. https://doi.org/10.1007/978-1-4419-7943-8

[10] Afanasenkov, A.N. (2002) Retonation Wave upon Shock-Wave Initiation of Detonation of Solid Explosives. *Combustion, Explosion and Shock Waves*, **38**, 470-472. https://doi.org/10.1023/A:1016271501868

[11] Jing, Q., Huang, J.X., Liu, Q.M., Chen, X., Wang, Z.S., Liu, C.Q., *et al.* (2021) The Flame Propagation Characteristics and Detonation Parameters of Ammonia/Oxygen in a Largescale Horizontal Tube: As a Carbon-Free Fuel and Hydrogen-Energy Carrier. *International Journal of Hydrogen Energy*, **46**, 19158-19170. https://doi.org/10.1016/j.ijhydene.2021.03.032

[12] Oppenheim, A.K., Laderman, A.J. and Urtiew, P.A. (1962) The Onset of Retonation.

Combustion and Flame, **6**, 193-197. https://doi.org/10.1016/0010-2180(62)90089-5

[13] Blomshield, F. (2007) Lessons Learned in Solid Rocket Combustion Instability. In 43*rd AIAA/ASME/SAE/ASEE Joint Propulsion Conference & Exhibit*, Cincinnati, 8-11 July 2007, 5803. https://doi.org/10.2514/6.2007-5803

[14] Shima, S., Nakamura, K., Gotoda, H., Ohmichi, Y. and Matsuyama, S. (2021) Formation Mechanism of High-Frequency Combustion Oscillations in a Model Rocket Engine Combustor. *Physics of Fluids*, **33**, Article ID: 064108. https://doi.org/10.1063/5.0048785

[15] Larsen, C.E. (2008) Nasa Experience with Pogo in Human Spaceflight Vehicles. NATO RTO Symposium ATV-152 on Limit-Cycle Oscillations and Other Amplitude-Limited, Self-Excited Vibrations, number RTO-MP-AVT-152.

[16] Poinsot, T. (2017) Prediction and Control of Combustion Instabilities in Real Engines. *Proceedings of the Combustion Institute*, **36**, 1-28. https://doi.org/10.1016/j.proci.2016.05.007

[17] Connelly, T.A. and Kyritsis, D.C. (2015) Experimental Investigation of Flame Propagation in Long, Narrow, and Open Tubes. *Journal of Energy Engineering*, **141**, C4014016. https://doi.org/10.1061/(ASCE)EY.1943-7897.0000230

[18] Kerampran, S., Desbordes, D., Veyssiere, B. and Bauwens, L. (2001) Flame Propagation in a Tube from Closed to Open End. 39*th Aerospace Sciences Meeting and Exhibit*, Reno, 8-12 January 2001, 1082. https://doi.org/10.2514/6.2001-1082

[19] Ciccarelli, G. and Dorofeev, S. (2008) Flame Acceleration and Transition to Detonation in Ducts. *Progress in Energy and Combustion Science*, **34**, 499-550. https://doi.org/10.1016/j.pecs.2007.11.002

[20] Bennewitz, J.W. and Frederick, R.A. (2013) Overview of Combustion Instabilities in Liquid Rocket Engines-Coupling Mechanisms & Control Techniques. 49*th AIAA/ASME/SAE/ASEE Joint Propulsion Conference*, San Jose, 15-17 July 2013, 4106. https://doi.org/10.2514/6.2013-4106

[21] White, F.M. (2008) Fluid Mechanics. The McGraw Hill Companies, New York.

[22] Dunlap, R., Blackner, A.M., Waugh, R.C., Brown, R.S. and Willoughby, P.G. (1990) Internal Flow Field Studies in a Simulated Cylindrical Port Rocket Chamber. *Journal of Propulsion and Power*, **6**, 690-704. https://doi.org/10.2514/3.23274

[23] Candel, S.M. (1992) Combustion Instabilities Coupled by Pressure Waves and Their Active Control. *Symposium* (*International*) *on Combustion*, **24**, 1277-1296. https://doi.org/10.1016/S0082-0784(06)80150-5

[24] de Jong, C.A.F. (1995) Analysis of Pulsations and Vibrations in Fluid-Filled Pipe Systems. *Proceedings of the ASME* 1995 *Design Engineering Technical Conferences Collocated with the ASME* 1995 15*th International Computers in Engineering Conference and the ASME* 1995 9*th Annual Engineering Database Symposium*. *Volume* 3*B*: 15*th Biennial Conference on Mechanical Vibration and Noise—Acoustics, Vibrations, and Rotating Machines*, Boston, 17-20 September 1995, 829-834. https://doi.org/10.1115/DETC1995-0478

[25] Li, X., Zhou, N., Liu, X.Y., Huang, W.Q., Chen, B. and Rasouli, V. (2020) Numerical Simulation of the Influence of Pipe Length on Explosion Flame Propagation in Open-Ended and Close-Ended Pipes. *Science Progress*, **103**, 1-24. https://doi.org/10.1177/0036850420961607

[26] Kao, S. and Shepherd, J.E. (2008) Numerical Solution Methods for Control Volume Explosions and ZND Detonation Structure. GALCIT Report FM2006.007, 1-46. https://citeseerx.ist.psu.edu/document?repid=rep1&type=pdf&doi=10362e38f68752e9f79768ba1ef36ad7a22b0879